Tidal Volume and Instantaneous Respiration Rate Estimation using a Volumetric Surrogate Signal Acquired via a Smartphone Camera

Bersain A. Reyes, *Student Member, IEEE*, Natasa Reljin, Youngsun Kong, *Student Member, IEEE*, Yunyoung Nam, *Member, IEEE*, and Ki H. Chon, *Senior Member, IEEE*

***Abstract*—Two parameters that a breathing status monitor should provide include tidal volume (V_T) and respiration rate (RR). Recently, we implemented an optical monitoring approach that tracks chest wall movements directly on a smartphone. In this paper, we explore the use of such noncontact optical monitoring to obtain a volumetric surrogate signal, via analysis of intensity changes in the video channels caused by the chest wall movements during breathing, in order to provide not only average RR but also information about V_T and to track RR at each time instant (IRR). The algorithm, implemented on an Android smartphone, is used to analyze the video information from the smartphone's camera and provide in real time the chest movement signal from $N = 15$ healthy volunteers, each breathing at V_T ranging from 300 mL to 3 L. These measurements are performed separately for each volunteer. Simultaneous recording of volume signals from a spirometer is regarded as reference. A highly linear relationship between peak-to-peak amplitude of the smartphone-acquired chest movement signal and spirometer V_T is found ($r^2 = 0.951 \pm 0.042$, mean $\pm$ SD). After calibration on a subject-by-subject basis, no statistically significant bias is found in terms of V_T estimation; the 95% limits of agreement are -0.348 to 0.376 L, and the root-mean-square error (RMSE) was 0.182 ± 0.107 L. In terms of IRR estimation, a highly linear relation between smartphone estimates and the spirometer reference was found ($r^2 = 0.999 \pm 0.002$). The bias, 95% limits of agreement, and RMSE are -0.024 breaths-per-minute (bpm), -0.850 to 0.802 bpm, and 0.414 ± 0.178 bpm, respectively. These promising results show the feasibility of developing an inexpensive and portable breathing monitor, which could provide information about IRR as well as V_T, when calibrated on an individual basis, using smartphones. Further studies are required to enable practical implementation of the proposed approach.**

***Index Terms*—Optical monitoring, respiration rate, smartphone camera, tidal volume, time-frequency analysis, volume surrogate.**

Manuscript received August 21, 2015; revised December 14, 2015 and February 15, 2016; accepted February 18, 2016. Date of publication February 23, 2016; date of current version May 3, 2017. This work was supported in part by the U.S. Army Medical Research and Material Command (US-AMRMC) under Grant W81XWH-12-1-0541.

B. A. Reyes, N. Reljin, and K. H. Chon are with the Department of Biomedical Engineering, University of Connecticut, Storrs, CT 06269 USA (e-mail: bareyes@engr.uconn.edu; reljin@engr.uconn.edu; kchon@engr.uconn.edu).

Y. Kong and Y. Nam are with the Department of Computer Science and Engineering, Soonchunhyang University, Asan 336-745, Korea (e-mail: vengeful224@gmail.com; yynams@gmail.com).

Digital Object Identifier 10.1109/JBHI.2016.2532876

I. Introduction

MONITORING of respiration status has been recognized as critical to identifying and predicting serious adverse events [1], [2]. Two basic parameters that a breathing monitor should be able to provide are tidal volume (V_T) and respiration rate (RR) [3]. V_T provides information about the respiration depth and is defined as the volume of air moved with each breath; on the other hand, RR corresponds to the number of breaths per unit of time and is commonly expressed in breaths-per-minute (bpm). In turn, the product of these two quantities defines the volume of gas moved by the respiratory system per minute, called minute ventilation ($\dot{V}_E$). Normal average values for a human are around 0.5 L and 12 breaths per minute (bpm) for V_T and RR, respectively. These values are not fixed and the mechanism of respiratory control is crucial in determining $\dot{V}_E$ by adjusting the combination of V_T and RR according to a body's requirements in response to different scenarios [4].

Current clinical continuous RR monitoring methods include qualified human observation, transthoracic impedance, inductance plethysmography, capnography monitoring, and tracheal sound monitoring [5]–[8]. Each method has its own disadvantages, e.g., it is time consuming and subjective to do human observation and patients have a low tolerance for using the nasal cannula in capnography [3]. However flawed, at least clinical devices exist for monitoring. Outside clinical or research settings, there is still a lack of monitoring devices that can very accurately determine RR in a noninvasive way, to be used on a daily basis.

Regarding V_T measurement, current clinical methods include spirometry, impedance pneumography, inductance plethysmography, photoplethysmography, computed tomography, phonospirometry, Doppler radar, and more recently, electrocardiography [9]–[17]. Similar to RR estimation, limitations arise while estimating V_T, e.g., high doses of ionizing radiation in computed tomography, or causing alteration in both natural RR and V_T due to spirometer use [18]. Moreover, having been designed for clinical settings or research centers, these methods employ specialized devices that are not translated easily to everyday use due to their high costs, need for skilled operators, or limited mobility.

Nowadays, smartphones are widely available and vital sign applications have been found to be accurate and robust. In addition, smartphones have fast microprocessors and large data stor-

age and media capabilities, which make them an enticing option for developing a ubiquitous mobile respiration monitoring system. In an attempt to develop such a mobile system, we analyzed an acoustical approach and found good correlation between the smartphone-based RR estimates and the spirometer-based ones ($r^2 \approx 0.97$), as well as 95% limits of agreement ranging approximately from -1.4 to 1.6 bpm for a breathing range from 15 to 35 bpm [19]. However, the last approach requires plugging an additional acoustical sensor into the smartphone in order to extract information from tracheal sounds and just provides estimates of RR and breath-phase onset.

In order to overcome the need for an external sensor for the task of RR estimation, i.e., the acoustical sensor, more recently our research group studied a noncontact optical approach that takes advantage of a smartphone's cameras. In particular, an algorithm that allows the real-time acquisition of a surrogate volumetric signal from breathing-related light intensity changes due to chest wall movements was implemented on a smartphone and its performance was tested in healthy volunteers breathing at a metered pace and spontaneously, while seated. Under the paced breathing, we found that the smartphone-based estimates of average RR were accurate when compared to those obtained from inductance plethysmography.

In general, the noncontact optical breathing monitor employs a video camera placed at distance from the subject's body to capture the intensity changes of the reflected light caused by his or her chest wall movements as they modify the path length of the illumination light [20]. The chest wall movements also change the amount of light reflected back to the video camera. During inspiration, the inspiratory muscles contract, resulting in an enlarged thoracic cavity; the diaphragm descends downward increasing the vertical dimension, while the external intercostal muscles elevate the ribs and move the sternum upward and outward increasing the thoracic cavity in the horizontal axis. Due to this contraction, the lungs expand to fill the larger thoracic cavity, resulting in a drop of the intra-alveolar pressure that causes a flow of air into the lungs until the intra-alveolar pressure equals the atmospheric pressure [21]. The inspiratory muscles relax during the expiration, restoring the chest wall and stretched lungs to their preinspiratory sizes, due to their elastic properties, and causing a rise in the intra-alveolar pressure above atmospheric level forcing the air to leave the lungs [21]. Note that in the noncontact optical respiratory monitoring approach, volume changes are not directly measured but a surrogate signal is obtained from the analysis of the variations in the reflected light due to chest wall movements captured by the system's camera while breathing.

There have been efforts to perform respiratory monitoring via the noncontact optical approach described earlier, but most of them have solely focused on average RR estimation [20], [22]–[27]. Still, noncontact optical methods have been proposed for V_T estimation, which is more challenging than average RR estimation. In particular, chest wall surface markers tracked by an optical reflectance system have shown promising results [23]. Those findings have been supported by studies that showed a one-to-one relationship between changes of the external torso and V_T corresponding to internal lung air content [13]. More recently, a webcam and an image processing technique based on the detection of shoulder displacements were implemented for breathing pattern tracking [25]. However, to the best of our knowledge, a smartphone-based system that uses a noncontact optical approach together with an algorithm implemented directly in the smartphone for the task of V_T estimation is not available yet.

Further observation of the smartphone-acquired signals during our previous study pointed us to the possibility of obtaining more valuable information than the average RR. Namely, we noticed that our algorithm was capable of monitoring the increased amplitude of the chest movements when volunteers took deeper breaths.

In this paper, we propose a mobile system based on a noncontact optical approach implemented in a smartphone that provides information, from a volume surrogate, about both RR at each time instant (IRR) as well as V_T (when calibrated), in contrast to just average RR. For this study, the proposed respiratory monitoring system was implemented on a commercially available Android smartphone but could, of course, be implemented in smartphones using other operating systems. We collected signals from healthy volunteers and tested the performance of the proposed smartphone system for the tasks of IRR and V_T estimation, using the spirometer-acquired volume signal as reference.

II. Materials and Methods

A. Subjects

For this study, 15 ($N = 15$) healthy and nonsmoker volunteers (14 males and 1 female) aged 19–52 years (mean $\pm$ standard deviation: 28.73 ± 9.27), weight 70.14 ± 19.83 kg, and height 175.67 ± 5.94 cm, were recruited. Exclusion criteria included individuals with previous pneumothorax, those with chronic respiratory illnesses such as asthma, and anyone who was currently ill with the common cold or an upper respiratory infection. The group of volunteers consisted of students and staff members from the University of Connecticut (UConn), USA. Each volunteer consented to be a subject and signed the study protocol approved by the Institutional Review Board of UConn.

B. Respiration Signals Acquisition

1) Equipment: The HTC One M8 smartphone (HTC Corporation, New Taipei City, Taiwan) running the Android v4.4.2 (KitKat) operating system was selected for this research as it is one of the state-of-the-art Android smartphones, which is nowadays the dominant operating system worldwide in mobile devices. The HTC One M8 allows simultaneous dual camera recording supported by its processor running a 2.3 GHz quad-core CPU (Snapdragon 801, Qualcomm Technologies Inc., San Diego, CA, USA). For this study, the chest movement signal of interest was collected via the frontal camera consisting of a 5 MP, backside-illumination sensor with wide angle lens and 1080p full HD video recording capabilities at 30 frames per second. The video recording was processed in real time using an application specifically designed for and implemented in the smartphone to obtain a volumetric surrogate signal, referred to in this paper as the chest movement signal, of the subject as discussed in the next section. After finishing the maneuver, the

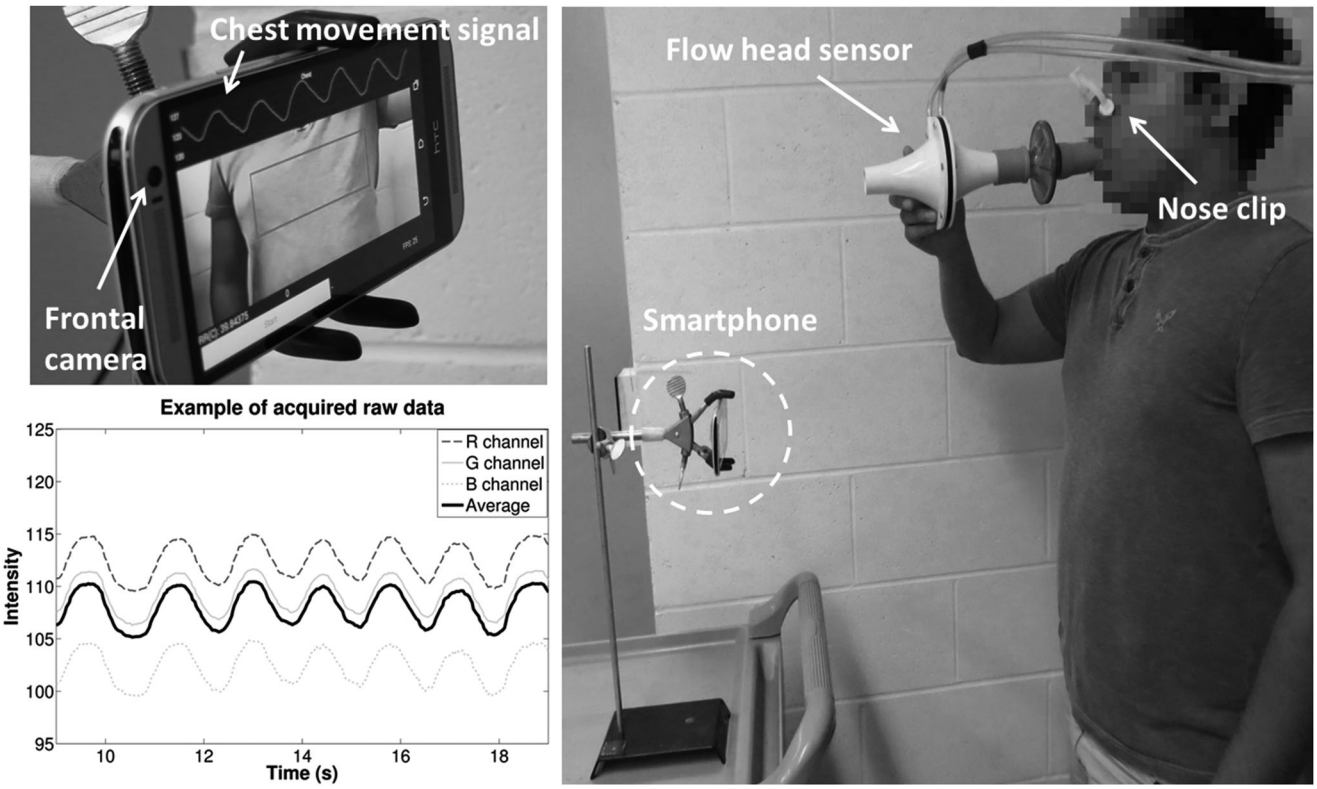

Fig. 1. Recording of chest movement signal using a smartphone's camera and volume using a spirometer during a respiration maneuver. The smartphone was placed in front of the subject at thorax level in order to record chest movements which were later compared to the reference volume signal from the spirometer. *Top left panel:* Zoomed view of the developed smartphone app. *Bottom left panel:* A segment of the raw signals extracted from the RGB channels and their average.

chest movement signal and the corresponding time vector were saved into a text file in the smartphone and transferred to a personal computer for off-line analysis of results using MATLAB (R2012a, The Mathworks, Inc., Natick, MA, USA).

Together with the smartphone-recorded volumetric surrogate signal, a spirometer system consisting of a respiration flow head connected to a differential pressure transducer to measure airflow was used to record the airflow signal (MLT1000L, FE141 Spirometer, ADInstruments, Inc., Dunedin, New Zealand). The volume signal, regarded as reference for V_T and IRR estimation, was computed in the phone as the integral of the airflow over time. Both the airflow and volume signals were sampled at 1 kHz using a 16-bit A/D converter (PowerLab/4SP, ADInstruments, Inc.). A 3.0 L calibration syringe (Hans Rudolph, Inc., Shawnee, KS, USA) was used to calibrate the spirometer system prior to recording of each volunteer. A new set consisting of disposable filter, reusable mouthpiece, and disposable nose clip was given to each volunteer (MLA304, MLA1026, MLA1008, ADInstruments, Inc.).

2) Acquisition Protocol: Each maneuver lasted approximately 2 min during which the volunteers were asked to breathe through the spirometer system at different volume levels ranging from around 300 mL to 3 L, depending on what was manageable for that individual. Each subject was instructed to breathe while first increasing his or her V_T with each breath for around 1 min and then decreasing his or her V_T with each breath for the remaining time. To provide visual feedback of the maneuver to the volunteers, their volume signal was displayed on a $40''$ monitor placed in front of them. Nose clips were used to clamp the nostrils during the respiration maneuver. Subjects were standing still during signal collection. The smartphone was positioned in front of the subject at approximately 60 cm in a three-pronged clamp placed at thorax level so that the frontal camera recorded chest wall movements associated with breathing during the maneuver. All signals were recorded in a regular dry lab with the ambient light, which predominantly consisted of ordinary fluorescent lamps located in the ceiling approximately 2.5 m above floor level and to a lesser extent, sunlight entering through the lab's windows. Although the smartphone and spirometer recordings were simultaneously started, 5 s of the initial and final apnea segments were acquired for automatic alignment purposes between both recordings. After initial apnea, subjects took a forced respiration cycle before performing the described respiration maneuver. Fig. 1 shows an example of the experimental setup. It is worth mentioning that volunteers were not restricted in wearing any color/pattern of their clothes during the maneuvers but instructed not to wear loose clothes.

C. Chest Movement Recording Algorithm

The two major anatomical contributors to the visibility of breathing are the rib cage and abdomen compartments of the chest wall, whose movements in the anteroposterior direction

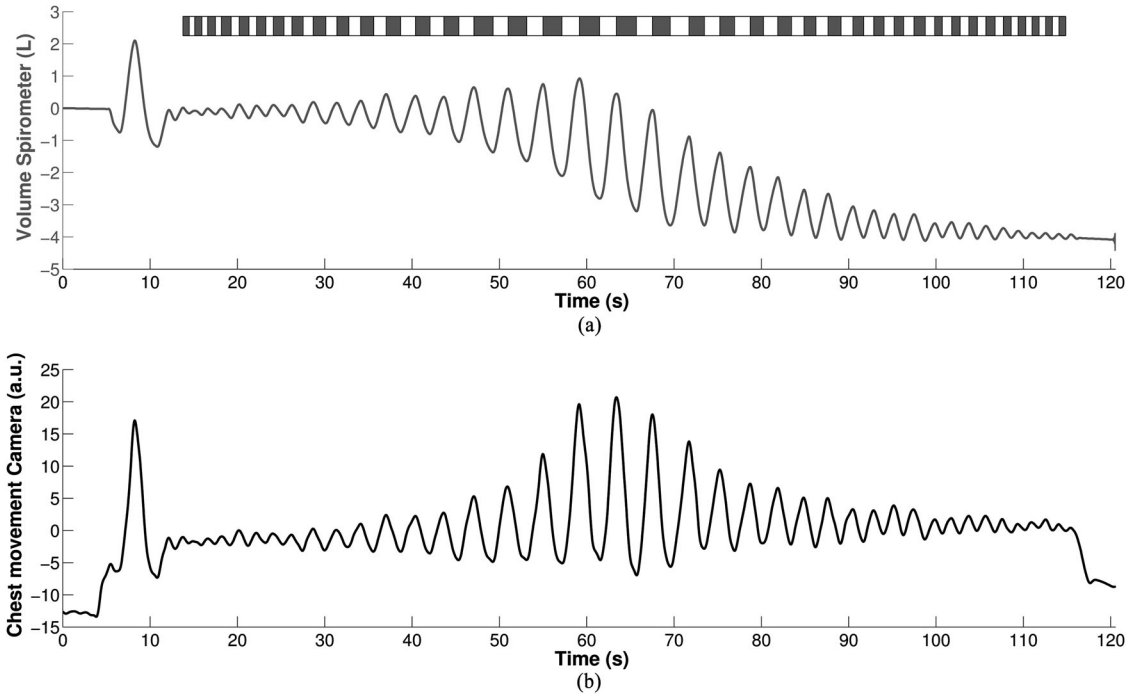

Fig. 2. Example of the acquired signals during the respiration maneuver of one subject. (a) Volume signal from spirometer. (b) Chest movement signal from smartphone's camera. Positive and negative deflections in the volume signal correspond to the inspiratory and expiratory phases and are indicated by light and dark gray bars displayed on top of the signals, respectively.

are greater than those in the vertical or transverse directions, with an increase of around 3 cm in the anteroposterior diameter over the vital capacity range [28]. There is a relationship between volume displacement and linear motion during breathing [28], and a one-to-one relationship between changes of the external torso and tidal volume corresponding to internal lung air content has been found [13]. The proposed smartphone algorithm is intended to take advantage of this relationship to obtain a volumetric surrogate by analyzing the changes in the intensity of the reflected light caused by the breathing-related chest wall movements captured at a distance with a smartphone's camera. In particular, the algorithm processes video recordings in real time, where at each time instant t, the intensities of the red, green and blue (RGB) channels are averaged within a rectangular region of interest (ROI) according to

$$I(t) = \left(\frac{1}{3D}\right)\left(\sum_{\{m,n\}\in \mathrm{ROI}} i_R(m,n,t) + \sum_{\{m,n\}\in \mathrm{ROI}} i_G(m,n,t) + \sum_{\{m,n\}\in \mathrm{ROI}} i_B(m,n,t)\right) \quad (1)$$

where $i_x(m,n,t)$ is the intensity value of the pixel at the mth row and nth column of the red, green, or blue channel within the ROI containing a total of D pixels. For this study, a region of 49×90 pixels were selected in a resolution of 320×240 pixels and focused on the thoracic area of the subject. This reduced resolution and ROI size were selected so that they do not compromise the sampling rate during the real-time monitoring in the smartphone app. With these settings, the frame rate dropped to around 25 frames per second. The average intensity waveform $I(t)$ was regarded as the chest movement signal, i.e., the volume surrogate, from which the tidal volume and respiratory rates were estimated. As shown in Fig. 1, despite the dc values, all channels carry similar information, and hence, their average was taken to avoid channel selection. An example of the raw volume acquired with a spirometer and the corresponding chest movement signal acquired online with the smartphone's camera and chest movement app is shown in Fig. 2 for the respiration maneuver performed by one subject. It should be noted that similar to other monitoring methods, e.g., inductance plethysmography, the proposed noncontact optical approach via the smartphone-acquired volumetric surrogate signal might be very weak if the clothes worn by the subject are not tight to his or her thorax, which can result in increased estimation errors of breathing parameters.

D. Data Preprocessing

The acquired chest movement signal was interpolated at 25 Hz via a cubic spline algorithm to achieve a uniform sampling rate that corrects fluctuations around this value during the online acquisition in the smartphone. The reference volume signal was downsampled to 25 Hz to achieve the same sampling frequency as the chest movement signal. In order to minimize high-frequency components not related to the respiration maneuver, the chest movement and reference volume signals were filtered with a fourth-order Butterworth lowpass filter at 2 Hz that was applied in a forward and backward scheme to produce zero-phase distortion and minimize the start and end transients.

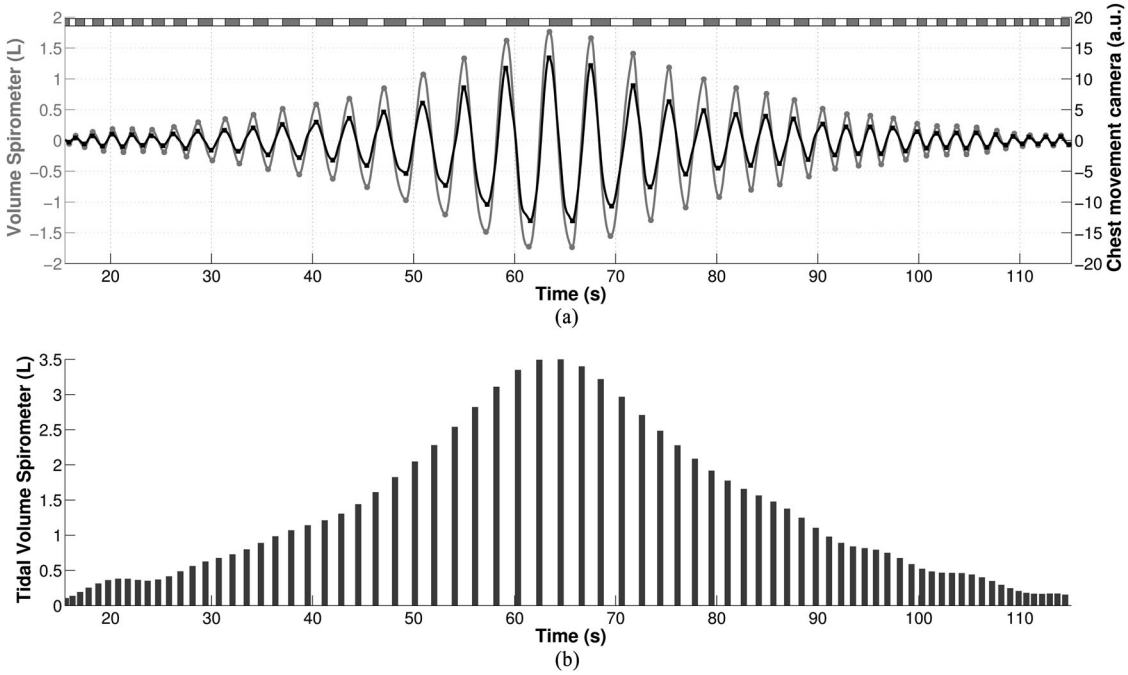

Fig. 3. Example of pre-processed signals during the respiration maneuver of one subject. (a) Detrended versions of a volume signal from the spirometer and the chest movement signal from a smartphone camera. Gray and black dots indicate the maxima and minima of volume and chest movement signals, respectively. (b) Tidal volume of each respiration phase computed as the absolute difference between the volumes at two consecutive breath-phase onsets.

After filtering, the chest movement and reference volume signals were automatically aligned using the cross-correlation function, where 20 s in the central portion of the maneuver were extracted from each recording to compute the cross-correlation sequence in order to obtain the sample lag providing the maximum cross-correlation value that indicates the required samples to be shifted. This alignment was required because of different starting times and delays of the smartphone and A/D converter acquisition systems during the simultaneous recording of the maneuver. The duration of the signals was set accordingly, to the minimum duration of both types of recordings.

Finally, both signals, the surrogate and the actual volume, were detrended via the empirical mode decomposition (EMD) method [29]. The essence of this decomposition is to identify the intrinsic oscillatory modes, called IMFs, of a signal through the time scales present in it. Its principal attractiveness resides in obtaining the IMFs directly from the signal without the use of any kernel, i.e., EMD depends only on the data. All the IMFs of the signal $s(t)$ under analysis are extracted automatically by a shifting process intended to eliminate riding waveforms and to produce close to zero mean value as defined by upper and lower envelope signals.

The EMD sifting process allows representation of the original signal in terms of its extracted components as

$$s(t) = \sum_{k=1}^{K} \mathrm{IMF}_k(t) + r_K(t) \tag{2}$$

where K is the total number of IMFs, and $r_K(t)$ is the residual signal. EMD has the characteristic of being a complete decomposition [29].

As shown in Fig. 2, the acquired reference volume from the spirometer and the chest wall movement signal from the smartphone camera, consist of a slowly varying trend superimposed on the fluctuating breathing signal of interest. As a result of the sifting process, the first IMFs contain the lower scales (higher frequency components), while the trend is contained in the last IMFs. Hence, the selection of the appropriate IMFs was based on the mean of the fine-to-coarse EMD reconstruction by observing the evolution of the empirical mean of the reconstructions as a function of the test order (K), and identifying the order at which it departs significantly from zero [30]. A flowchart of the signal preprocessing stage is shown in Fig. 4(a).

E. Tidal Volume Estimation Using Smartphone Camera Signal

The volume signal from the spirometer was used to automatically determine the breath-phase onsets during the maneuver by finding their local maxima and minima. Inspiratory and expiratory phases corresponded to positive and negative traces of the volume signal, respectively. V_T of each phase was computed as the absolute volume difference between two consecutive breath-phase onsets. The time location of the onsets was used to determine the corresponding maxima or minima in the aligned chest movement signal around a time window of 500 ms centered at each breath-phase onset. The amplitude difference between two consecutive breath-phase onsets in the chest movement signal was used for V_T estimation via the smartphone.

For calibration, a least-squares linear regression between the reference V_T and the absolute peak-to-peak amplitude of chest movement was performed for each subject; half of the data points of the maneuver were randomly selected for

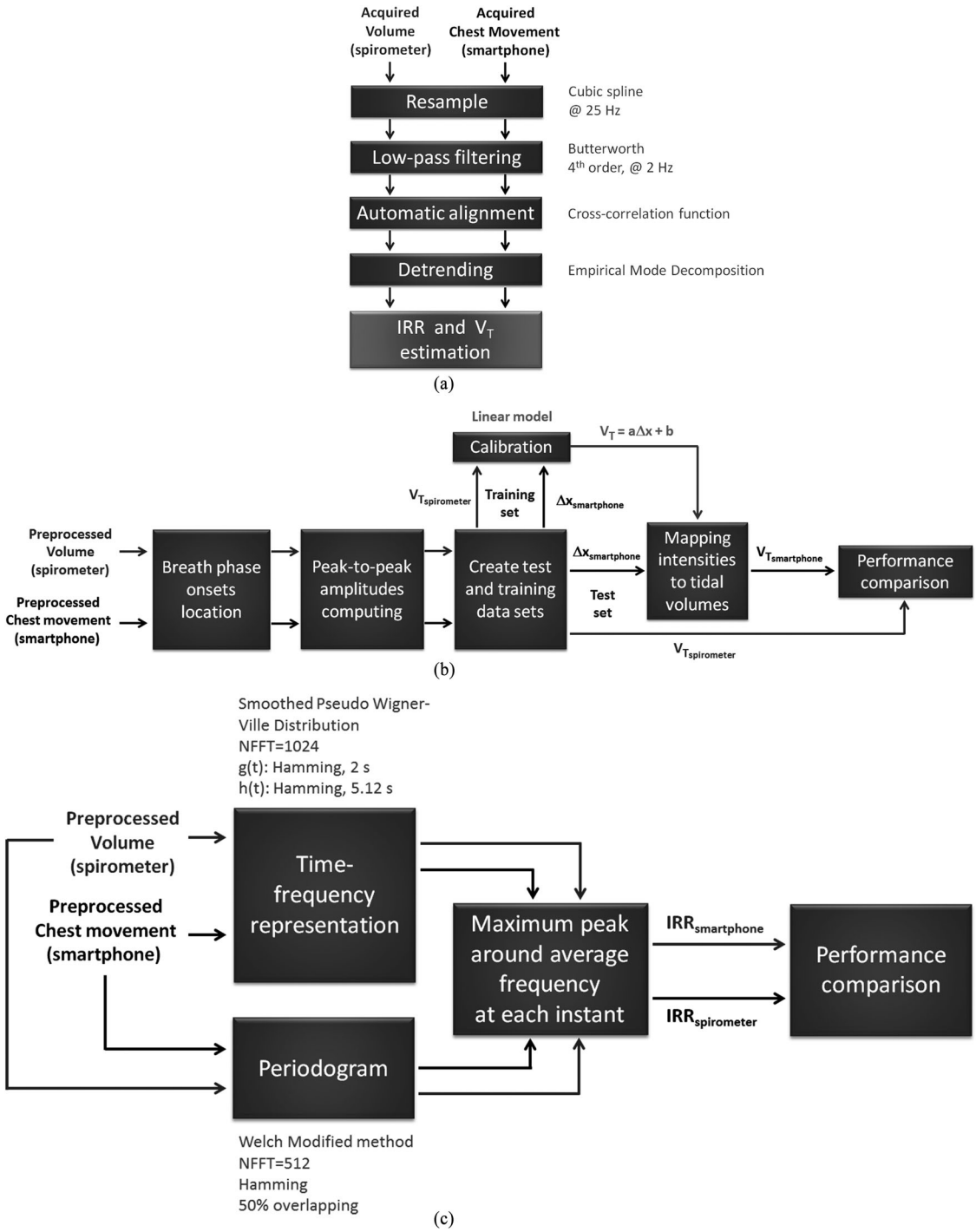

Fig. 4. Flowcharts of the signal processing used for tidal volume (V_T) and instantaneous RR (IRR) estimation using smartphone-acquired chest movements. (a) Signal preprocessing procedure. (b) Tidal volume estimation procedure. (c) Instantaneous RR estimation procedure.

calibration purposes and regarded as a training data set, while the remaining half were used as a test data set to which the computed linear model was applied in order to map the smartphone-based measurements to volume estimates in liters.

The performance of the V_T estimation was measured on the test data using the regression parameter r^2, the root-mean-square error (RMSE), and the normalized RMSE (NRMSE), defined as follows:

$$\text{RMSE} = \sqrt{\frac{\sum_{i=1}^{M}\left(V_{T_{\text{spirometer}}}(i) - V_{T_{\text{smartphone}}}(i)\right)^2}{M}} \tag{3}$$

$$\text{NRMSE} = \frac{\text{RMSE}}{\text{mean}\left(V_{T_{\text{spirometer}}}\right)} \cdot 100\% \tag{4}$$

where $V_{T_{\text{spirometer}}}$ indicates the tidal volume obtained from the spirometer-acquired volume signal, $V_{T_{\text{smartphone}}}$ the tidal volume estimated from smartphone-acquired chest movements after calibration, and M is the number of breath phases of the analyzed maneuver used for testing. A flowchart of the tidal volume estimation stage is shown in Fig. 4(b).

Fig. 3(a) shows an example of the preprocessed reference volume and chest movement signals. The breath-phase onsets and respiration phases as computed from the volume signal are indicated on top. The corresponding maxima and minima are superimposed on each signal. The detrended versions of the spirometer and smartphone signals shown in Fig. 2 are shown in Fig. 3(a), after applying the EMD approach. Note that although the inspiratory and expiratory phases of the maneuver can be noticed in both types of acquired signals as positive and negative segments in Fig. 2, the signal detrending stage simplifies their further processing. In Fig. 3(b), the reference V_T is shown for every respiratory phase of the respiration maneuver displayed in Fig. 3(a), where tidal volumes were computed as the absolute volume differences between two consecutive breathing onsets.

F. Instantaneous RR Estimation Using Smartphone Camera Signal

To estimate IRR from the smartphone-acquired chest movement signal, a time-varying spectral technique was used. In this paper, the smoothed pseudo-Wigner-Ville distribution (SPWVD) time-frequency representation (TFR) was employed. A TFR is a function that simultaneously describes the energy density of a signal in the time and frequency domains, allowing one to analyze which frequencies of a signal under study are present at a certain time [31]. Then, TFR analysis is useful for analyzing signals whose frequency content varies over time, as is the case with respiration signals. Note that the use of a simple peak detector would be an option for estimating the instantaneous respiratory rates. However, due to low sampling rates and not-well-defined breathing peaks, all simple peak detectors result in less accurate respiratory rate estimation than do time-varying spectral approaches. WVD belongs to the Cohen's class of bilinear TFRs; it possesses several interesting properties, and in particular provides the highest time-frequency resolution. However, the main limitation of the WVD is the presence of cross-terms that obscure its readability. Several techniques have been proposed to reduce the number of cross-terms of the WVD; however, there is a tradeoff between the amount of cross-term interference and the time-frequency resolution. The spectrogram is one such attempt, a joint time-frequency smoothing window is applied and hence the performance in one direction is enhanced at the expense of degrading the performance in the other. In contrast, the SPWVD employs independent time and frequency smoothing windows [32], as given by

$$\text{SPWVD}\,(t,f) = \int_{-\infty}^{\infty} h(\tau) \int_{-\infty}^{\infty} g(\eta - t) \cdot s\left(\eta + \frac{\tau}{2}\right) \cdot s^{*}\left(\eta + \frac{\tau}{2}\right) d\eta e^{-j2\pi f\tau} d\tau \quad (5)$$

TABLE I
DISTRIBUTION OF BREATHING CYCLES, TIDAL VOLUME, AND RR MEASURED BY SPIROMETER DURING BREATHING MANEUVERS ($N = 15$ SUBJECTS)

Parameter	Min	Max	Average
Breathing cycles (cycles)	16	51	31.40 ± 10.25
Maneuver tidal volume (L)	0.24 ± 0.11	3.11 ± 0.67	1.32 ± 0.26
Maneuver RR (bpm)	11.08 ± 3.69	35.45 ± 13.04	17.12 ± 5.28

Values presented as mean $\pm$ standard deviation.

where $s(t)$ is the signal under analysis, $g(\cdot)$ is the time smoothing window, and $h(\cdot)$ is the frequency smoothing window in the time-domain [33].

The SPWVD was applied to the volume and chest movement signals. The SPWVD was computed using $\text{NFFT} = 1024$ frequency bins, a 2-s Hamming window as the time-smoothing window, and a 5.12-second Hamming window as the frequency-smoothing window. After computing, the SPWVD was normalized between [0–1]. The Welch-modified periodogram was used to compute the spectrum of the whole maneuver in order to obtain the central or average respiration frequency as the maximum spectral peak. The periodogram was computed using 50% overlap, 512 frequency bins, and a Hamming window. Then, at each time instant, the maximum peak around the central frequency was computed and the frequency at which that maximum occurs was regarded as the respiration frequency at that instant so that a vector of instantaneous respiration frequency was returned from each SWPVD. The frequency vector extracted from the spirometer-based volume was regarded as the reference instantaneous respiration frequency and was compared against the frequency vector extracted from the corresponding smartphone-based chest movement signal. All instantaneous respiration frequencies were converted from hertz to bpm to obtain IRR. Note that the SPWVD is a well-known time-varying spectral approach, which can be implemented in a variety of programming languages including the one we have used for the smartphone app development, Java.

Similar to tidal volume estimation, the performance of the IRR estimation using the smartphone-acquired chest movement signal was tested using three performance indices by considering the IRR from volume signal as reference: the RMSE, the NRMSE, and the cross-correlation index ρ is defined as follows:

$$\rho = \frac{\sum_{i=1}^{S} \text{IRR}_{\text{spirometer}}(i) \cdot \text{IRR}_{\text{smartphone}}(i)}{\sqrt{\sum_{i=1}^{S} \left(\text{IRR}_{\text{spirometer}}(i)\right)^2 \cdot \sum_{i=1}^{S} \left(\text{IRR}_{\text{smartphone}}(i)\right)^2}} \quad (6)$$

where $\text{IRR}_{\text{spirometer}}$ indicates the IRR obtained from the spirometer-acquired volume signal, $\text{IRR}_{\text{smartphone}}$ is the IRR estimated from smartphone-acquired chest movements, and S is the number of samples of the analyzed signal, i.e., time instants. RMSE and NRMSE were computed via (3) and (4), by replacing the V_T values at each breath phase by the IRR values at each time instant. A flowchart of the IRR estimation stage is shown in Fig. 4(c).

TABLE II
INFORMATION RELATED TO THE BIOMETRICS, BREATHING MANEUVER, CALIBRATION MODEL, AND PERFORMANCE OF THE SMARTPHONE-BASED TIDAL VOLUME AND INSTANTANEOUS RR ESTIMATES IN COMPARISON TO THE REFERENCE SIGNAL FROM SPIROMETER FOR EACH OF THE $N = 15$ SUBJECTS

							Calibration Parameters for V_T Estimation			V_T Estimation Errors		IRR Estimation Errors	
Subject No.	Gender	Age (years)	Weight (kg)	Height (m)	Body Mass Index (kg/m^2)	Breathing Cycles	m	b	r^2	RMSE (L)	NRMSE (%)	RMSE (bpm)	NRMSE (%)
1	M	32	75	1.63	28.23	51	0.148	0.093	0.994	0.119	11.105	0.361	1.477
2	M	35	70	1.70	24.22	36	0.138	0.200	0.983	0.126	11.007	0.312	1.426
3	M	32	60	1.79	18.73	36	0.134	0.483	0.944	0.281	19.691	0.422	1.731
4	M	24	82	1.72	27.72	40	0.147	0.173	0.980	0.484	26.996	0.295	1.440
5	F	35	60	1.65	22.04	37	0.140	0.199	0.966	0.286	21.526	0.349	1.620
6	M	52	70	1.73	23.39	37	0.295	−0.131	0.984	0.261	16.038	0.288	1.898
7	M	26	77	1.77	24.58	31	0.076	0.206	0.981	0.064	9.371	0.343	1.845
8	M	25	70	1.78	22.09	46	0.114	0.166	0.966	0.127	10.293	0.330	2.200
9	M	19	73	1.83	21.80	25	0.086	0.341	0.933	0.095	9.176	0.321	2.167
10	M	19	62	1.79	19.35	17	0.071	0.078	0.975	0.157	13.861	0.472	5.177
11	M	19	64	1.80	19.75	21	0.068	0.161	0.984	0.189	21.134	0.437	4.099
12	M	22	69	1.78	21.78	29	0.110	0.588	0.867	0.141	13.749	0.310	1.462
13	M	40	98	1.80	30.25	16	0.360	0.135	0.938	0.128	13.995	0.975	12.543
14	M	30	62	1.76	20.02	24	0.132	−0.231	0.850	0.134	13.628	0.621	4.061
15	M	21	88	1.82	26.57	25	0.092	−0.224	0.935	0.139	13.400	0.380	2.317
Mean		**28.73**	**70.14**	**1.76**	**23.37**	**31.40**	**0.141**	**0.149**	**0.952**	**0.182**	**14.998**	**0.414**	**3.031**
S.D.		**9.27**	**19.83**	**0.06**	**3.51**	**10.25**	**0.082**	**0.227**	**0.043**	**0.107**	**5.171**	**0.178**	**2.873**

III. RESULTS

The smartphone-acquired chest movement signal showed temporal amplitude variation related to the volume from spirometer during the breathing maneuver as shown in Fig. 2 and more evidently in Fig. 3 after detrending. In the following subsections we present the results in terms of tidal volume estimation and RR estimation using this smartphone-acquired chest movement signal. The distribution of the number of breathing cycles, average V_T, and average RR performed by the volunteers during the breathing maneuvers are shown in Table I. As can be seen, the maneuvers included a wide range of breathing cycles, rates and depths. Table II presents relevant information for all subjects concerning their biometrics, the corresponding calibration coefficients used for V_T estimation, and the comparison of the V_T and IRR smartphone-based estimates to the ones obtained from the reference signal from spirometry.

A. Tidal Volume Estimation Using Smartphone Camera Signal

Fig. 5 shows the relationship between the absolute peak-to-peak amplitude of chest movement acquired with the smartphone and the reference tidal volume acquired with the spirometer for each breath phase of the maneuver performed by one subject. As shown in this figure, the amplitude differences of smartphone-based chest movement signals linearly correlate to reference V_T from the spirometer. The regression parameter r^2 between the absolute peak-to-peak amplitude of chest movement and reference tidal volume was computed for all breath phases of each subject ($r^2 = 0.951 \pm 0.042$, mean $\pm$ SD). The corresponding boxplot for all subjects is also shown in Fig. 5. A strong linear relationship ($r^2 > 0.9$) was found between the smartphone-based estimates and the reference tidal volume from

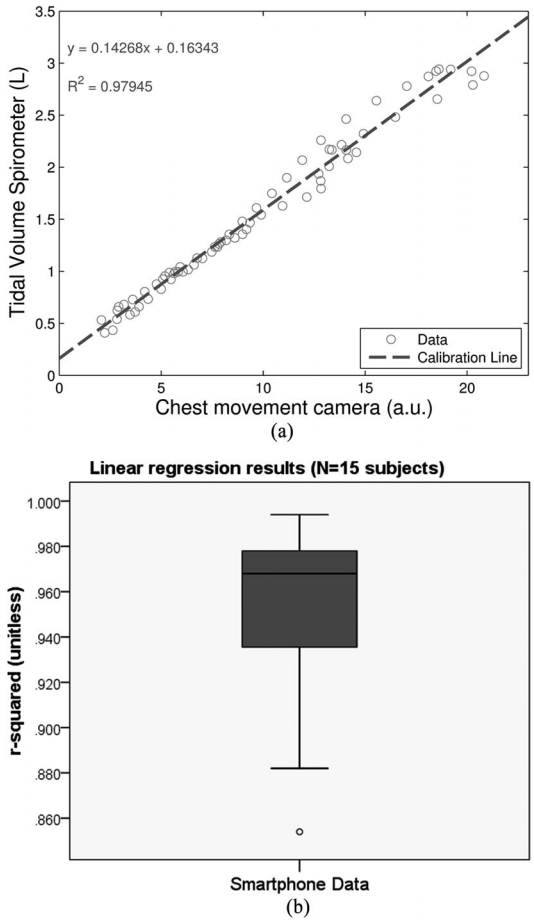

Fig. 5. Least-squares linear regression between the chest movement amplitude differences from smartphone and reference tidal volume from spirometer. (a) Example of regression for all data from one subject. (b) Boxplot of r^2 regression parameter for all subjects.

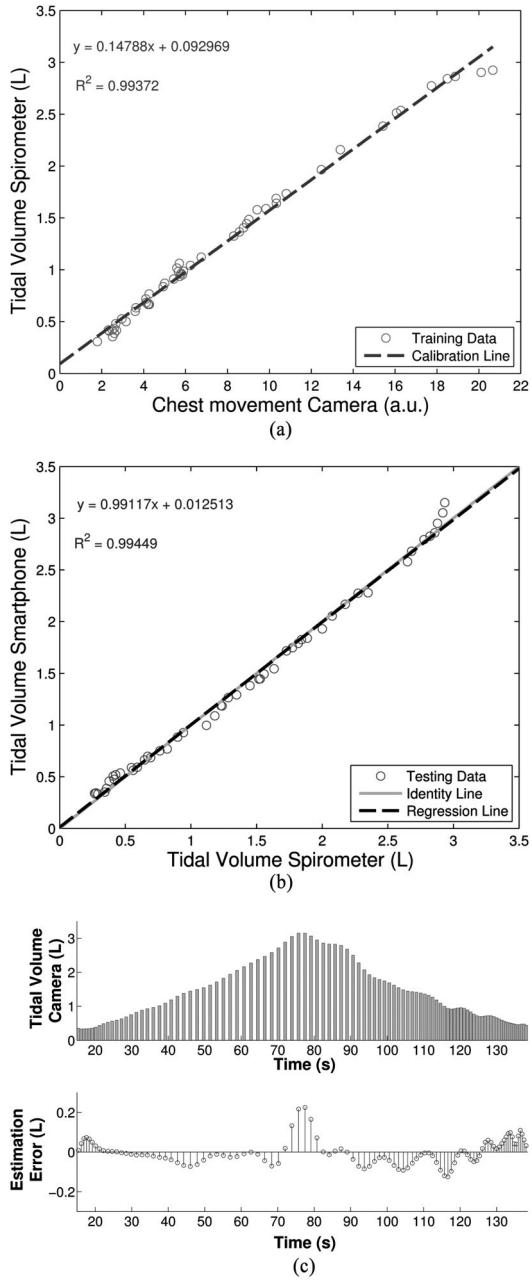

Fig. 6. Example of tidal volume estimation using a smartphone for one subject. (a) Calibration curve between chest movement amplitude differences from smartphone and tidal volume from spirometer for half of data randomly selected as training data. (b) Linear regression between smartphone-estimated tidal volume, after applying the calibration linear model, and reference tidal volume for the remaining half. (c) *Top:* Estimated tidal volumes from smartphone for each breath phase of the maneuver. *Bottom:* Corresponding differences between tidal volume derived from smartphone and reference tidal volume from spirometer throughout the whole breathing maneuver.

TABLE III
RESULTS OF TIDAL VOLUME ESTIMATION USING SMARTPHONE-ACQUIRED CHEST MOVEMENT SIGNALS COMPARED TO THE REFERENCE VOLUME FROM THE SPIROMETER ($N = 15$ SUBJECTS)

Parameter		Values		
r^2	(Unitless)	0.961	±	0.026
RMSE	(L)	0.182	±	0.107
NRMSE	(%)	14.998	±	5.171

Values presented as mean ± standard deviation.

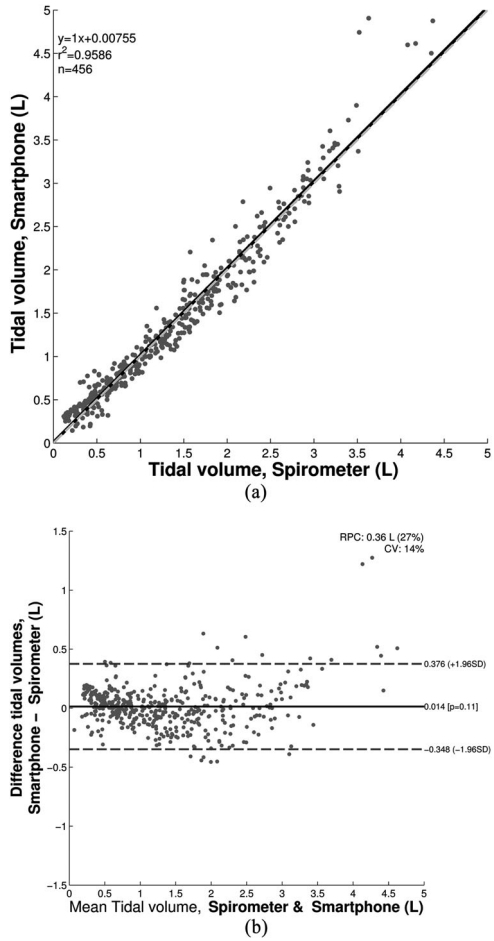

Fig. 7. Tidal volume estimation using smartphone ($N = 15$ subjects). (a) Regression curve. Gray dashed line indicates the identity line and the solid black the regression line. (b) Bland–Altman plot. Solid black line indicates the bias and dashed gray lines indicate the 95% limits of agreement.

the spirometer, as tested via a one-sample Wilcoxon signed rank test ($p = 6.41 \times 10^{-4}$) after the normality assumption did not hold (one-sample Kolmogorov–Smirnov test, $p = 0.002$).

An example of the V_T estimation procedure from smartphone-acquired data is shown in Fig. 6. From top to bottom, the first two plots of Fig. 6 correspond to the calibration process using the training data set [see Fig. 6(a)], and the testing process using the remaining randomly selected breath-phase data points [see Fig. 6(b)], respectively. The calibration parameters were computed via least-squares linear regression. Fig. 6(c) shows the corresponding smartphone-based V_T estimates, after using the calibration parameters, for each breath phase of the maneuver of one subject. The lower panel of Fig. 6(c) shows the corresponding error differences with respect to the reference V_T from spirometry.

The performance indices for smartphone-based V_T estimation are presented in Table III for the testing data set of all the

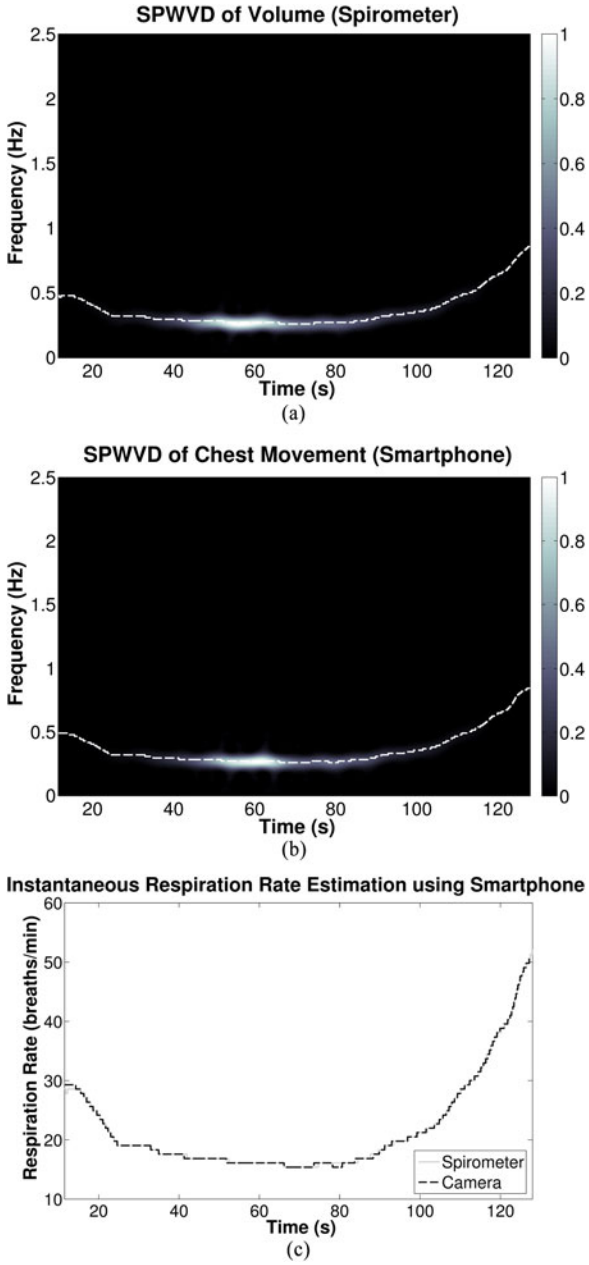

Fig. 8. Example of IRR estimation using smartphone-acquired chest movement signals. (a) SPWVD of the volume signal from the spirometer. (b) SPWVD of the chest movement signal from smartphone. White dashed lines indicate the maximum peak at each time instant. (c) Instantaneous RR computed from corresponding SPWVD of volume and chest movement signals.

TABLE IV
RESULTS OF THE INSTANTANEOUS RR ESTIMATION USING SMARTPHONE-ACQUIRED CHEST MOVEMENT SIGNAL COMPARED TO VOLUME SIGNAL FROM SPIROMETER ($N = 15$ SUBJECTS)

Parameter		Values		
ρ	(Unitless)	0.9992	±	0.0019
RMSE	(bpm)	0.414	±	0.178
NRMSE	(%)	3.031	±	2.873

Values presented as mean ± standard deviation.

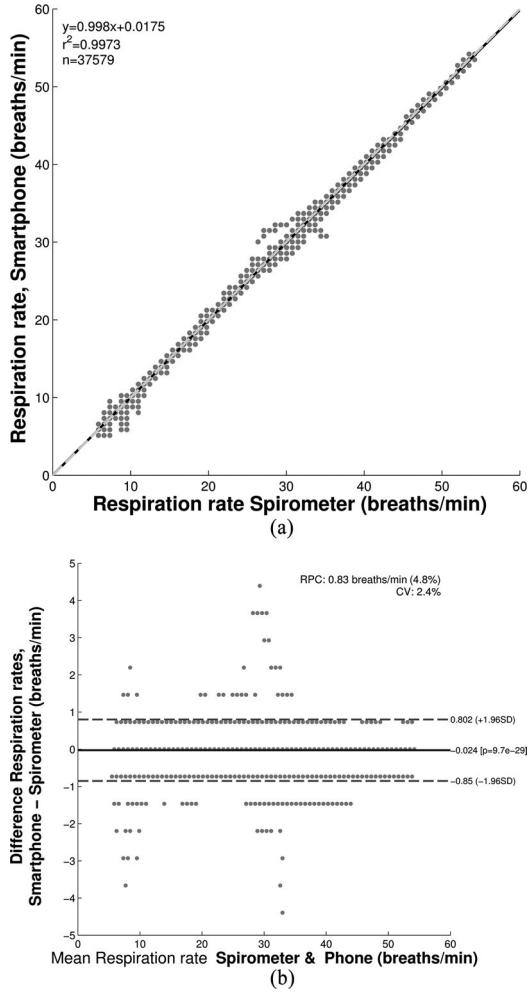

Fig. 9. Instantaneous RR estimation using smartphone ($N = 15$ subjects). (a) Calibration curve. Gray dashed line indicates the identity line and the solid black the calibration line. (b) Bland–Altman plot. Solid black line indicates the bias and dashed gray lines indicate the 95% limits of agreement.

volunteers, using the spirometer measurements as reference. The linear regression results shown in Fig. 6, for one subject, hold for all subjects, as shown in Fig. 7, when a linear regression was applied to all the tidal volume estimates from all volunteers. Fig. 7 also presents the corresponding Bland–Altman plot.

We found that when calibrated on a subject-by-subject basis, the smartphone-based V_T estimation produced a bias of 0.014 L and a standard deviation of 0.185 L, however the bias was not found to be statistically significant from a zero bias. Accordingly, the 95% limits of agreements were -0.348 to 0.376 L.

B. Instantaneous RR Estimation Using Smartphone Camera Signal

Fig. 8 shows an example of IRR estimation via the SPWVD technique applied to volume from a spirometer and chest movements from the smartphone for the respiration maneuver of one subject. The superimposed white dashed curve indicates the frequency at which the maximum energy of the SPWVD occurs at each time instant. Side-by-side comparison of the extracted IRR

from spirometer and smartphone signals is also presented. Observe that the subject was breathing at a faster pace than normal in order to account for the lower tidal volumes at the beginning and the end of the maneuver.

Table IV presents the performance indices of smartphone-based IRR estimation for all the subjects, using the spirometer values as reference. High cross-correlation coefficients were found between the IRR smartphone-based estimates and volume from spirometer. Fig. 9 reflects this high correlation as shown by the regression line parameters ($r^2 = 0.9973$). The corresponding Bland–Altman plot is also presented in Fig. 9. Compared to the spirometer, the bias $\pm$ standard deviation and the 95% limits of agreement were -0.024 ± 0.421 bpm and -0.850 to 0.802 bpm, respectively. Note that in this Bland–Altman plot, the IRR differences distribute at regular intervals given by the width of the frequency bins used in the calculation of the FFT during the time-frequency analysis, $\Delta = fs/2/\text{NFFT} = 0.0122$ Hz equivalent to $\Delta = 0.7324$ bpm.

IV. Discussion and Conclusion

In this paper we propose a smartphone-based respiration monitoring system for both instantaneous RR estimation and tidal volume estimation via an algorithm that tracks chest movements directly from a smartphone's camera. The HTC One M8 Android smartphone was used in this study and the algorithm was implemented in this device so that recordings of the chest movement signals were made directly on the phone. Together with this smartphone signal, airflow and volume signals were recorded with a spirometer and the latter was used as reference for IRR and V_T estimation. Recordings from fifteen healthy volunteers were obtained in a regular dry lab illuminated with fluorescent light while the volunteers were standing still and breathing at tidal volumes ranging from 300 mL to 3 L. Volunteers wore clothes with different colors and patterns. The developed algorithm can still detect the chest movements even if single color clothes are worn.

There have been several efforts to develop monitors that provide information about breathing status via optical approaches [20], [22]–[27], most of them monitoring only average RR. Recently, we implemented an algorithm that is able to track chest movements directly on a smartphone and found promising results in terms of average RR estimation. That study provided motivation to explore whether information beyond the average RR can be obtained from the smartphone-acquired chest movement signal. In particular, it appeared that the smartphone app provided a signal whose peak-to-peak amplitude was an indicator of the tidal volume of the volunteers. This *hypothesis* was corroborated in this study as exemplified in the recorded reference volume and chest movement signals, especially after detrending via EMD to remove existing drift in both signals. We also analyzed the correlation of the peak-to-peak amplitude of smartphone-acquired signals with the corresponding tidal volume signal acquired from a spirometer. We found that a strong correlation existed between the peak-to-peak amplitude of chest movement signals and tidal volume from the spirometer ($r^2 = 0.951 \pm 0.042$, mean $\pm$ SD). Given these correlation results, for each subject we randomly selected 50% of the data points for training the linear model during the calibration process, and the remaining 50% of the data for testing the tidal volume estimation based on the computed model. Once calibrated on an individual basis using the reference volume signal, when we mapped the chest movement amplitude differences at each breath phase of the testing data set, we found an RMSE of 0.182 ± 0.107 L which corresponded to $14.998 \pm 5.171\%$ when normalized to the mean value of the reference V_T of the testing data set of the maneuver. Overall, we found that a linear regression model fitted well the calibrated peak-to-peak amplitude of smartphone signals for the task of V_T estimation ($V_{T\text{smartphone}} = 1.005 \cdot V_{T\text{spirometer}} + 0.008$). We did not find statistically significant bias in the V_T estimation using smartphones and the 95% limits of agreement were -0.348 to 0.376 L. At this point it is difficult to state if this error estimate in tidal volume is acceptable for home monitoring use. Other popular methods for tidal volume estimation suffer from even higher estimation errors, for example, respiratory inductance plethysmography (RIP), when calibrated according to the manual (which usually states that 10% error difference is acceptable), often has much higher errors. Others have reported similar findings with respect to errors, e.g., Cohen *et al*. [5] found a bias and 95% limits of agreement in RIP sensors of approximately 0.4 L, and -0.3 to 1.1 L for a breathing range of 360 mL to 3.5 L. As noted in this work, the estimation error using RIP is even higher than our proposed approach using a smartphone's video camera.

By taking advantage of the high correlation between detrended smartphone signals and volume from the spirometer, we analyzed using the smartphone signal for the task of RR estimation at each time instant. Due to the time-varying characteristics of the signals, we employed the smoothed pseudo-WVD. We found high correlation between the smartphone-based IRR estimates and the spirometer-based values ($r^2 = 0.9992 \pm 0.0019$). We found an RMSE of 0.414 ± 0.178 bpm which corresponds to an NRMSE of $3.031 \pm 2.783\%$. The linear relationship between IRR estimated from the smartphone and IRR from reference volume was $\text{IRR}_{\text{smartphone}} = 0.9980 \cdot \text{IRR}_{\text{spirometer}} + 0.0175$. The 95% limits of agreement ranged from -0.850 to 0.802 bpm, while there was a statistically significant bias of -0.024 bpm. Other studies have reported the estimation of respiratory rate using noncontact optical approaches, e.g., in [22], the bias and standard deviation were found to be 0.19 and 2.46 bpm, respectively, in the range of approximately 10–70 bpm; in [24], the RMSE, bias, and standard deviation were 1.28, 0.12, and 1.33 bpm, respectively, in the range of approximately 10–22 bpm; in [25], the RMSE, bias, and 95% limits of agreement were 1.20, 0.02, and -2.40 to 2.45 bpm, respectively, in the range of approximately 10–24 bpm; while in [20], the RMSE, bias, and 95% limits of agreement were found to be 0.09, -0.02, and -1.69 to 1.65 bpm, respectively, in the range of approximately 7–24 bpm. Interestingly, the results reported in [20] during night conditions outperformed those mentioned earlier during daylight conditions. Although a straightforward comparison is not possible due to the differences in the measurement devices and the noncontact distance ranges tested, in general,

the current proposed noncontact optical monitoring of respiratory rate based on smartphones performs as well as, if not better than, the aforementioned studies.

Limitations of this study include the recording of the breathing maneuvers while the subjects were standing still, i.e., the subjects were instructed not to move. As found in other noncontact optical approaches, the main challenge arises from motion artifacts, especially when the dynamics of both the volumetric surrogate signal obtained from the chest wall movements and the motion artifacts have similar low-frequency ranges (< 2 Hz). Hence, it is expected that motion artifacts deteriorate the performance of the smartphone-based breathing estimates. Implementation of body tracking and artifact removal schemes similar to those reported in the literature to improve respiratory rate estimation [25], [34] are expected to reduce the effect of body motion not related to the breathing maneuver. Implementation and testing of such algorithms in the smartphone for respiratory monitoring, especially for the task of tidal volume estimation, should be explored in future studies.

Another major challenge is the variation of the ambient illumination at different times of the day due to fluctuations in the amount of sunlight, for example. The experiments presented in our study were performed at different times of the day and while the main illumination source came from the ceiling fluorescent lamps, the window shades of the laboratory were kept open or closed according to the needs of its users. Despite that, we did not notice that these variations disturbed the acquisition of the volumetric surrogate signal, perhaps due to the dominance of the fluorescent source. We recognize that systematic studies must analyze the performance of the proposed system in different levels of ambient illumination as well as to explore ways to account for these illumination variations.

The chest wall area of interest monitored during the breathing maneuver also represents another limitation. Classically, chest wall movements are attributed to two mechanical degrees of freedom due to contributions from rib cage and abdomen, which can be used to estimate tidal volume [28]. Although one-dimensional (1-D) or two-dimensional (2-D) displacements of these two compartments account for the majority of tidal volume, the algorithm ignores systematic effects of rib cage distortions [23]. In this study, the chest movement signal used as volume surrogate was extracted from an image's rectangular area centered on the anterior chest wall portion of the volunteer that visually provided the most dominant displacements while breathing. Accordingly, our approach ignores those small contributions due to rib cage distortions and only constructs the chest movement signal from the chest wall displacements monitored by the camera.

It is also expected that postural changes and airway obstruction impact the performance of the estimates, as has been found in other breathing monitor techniques [35], [36]. Postural changes can modify the contribution of the rib cage and abdomen compartments to tidal volume. A decreased rib cage excursion and an increased abdominal excursion have been found in the supine position compared to the sitting or standing postures [37], [38]. Accordingly, it is likely that another area of the thorax would provide a stronger surrogate signal when monitoring breathing in the supine position.

Another limitation is requiring subjects to wear fitted clothes during the experiments. As pointed out by other researchers, if the clothes are not tight enough to the subject's body a weak breathing-related signal might be obtained using the noncontact optical monitoring approach. Note that this is also the case in other respiratory monitoring methods based on chest wall displacements, like inductance plethysmography, where the sensors are recommended to be worn over bare skin or tight clothes. Observe that in general, the noncontact optical approach looks for changes in the light intensity due to the modification of the path length caused by breathing displacements of the chest wall, and is not limited to movements of clothing features. However, a systematic study is required to analyze the effect of wearing loose-fitting clothes. Finally, at this research point, note that to estimate tidal volume via the smartphone's camera, the measurement conditions should match those during which calibration was performed. Although we found that a linear model fitted well between peak-to-peak amplitude of chest movement signals from a smartphone and tidal volume from a spirometer, so that it can be used to calibrate the smartphone measurements to obtain tidal volume on an individual basis, a new calibration should be performed prior to acquisition if the subject's chest wall position monitored by the smartphone's camera displaces with respect to the one used for calibration. Other tidal volume estimation techniques suffer similar issues, *e.g.*, displacement of elastic belts wrapped around the rib cage and abdomen from the position employed when calibration was performed deteriorates the performance of the measurements in inductance plethysmography.

Several monitoring techniques for breathing status in clinical and research settings currently exist. This study and similar works are steps toward the developing of an inexpensive and mobile respiratory monitoring system that can be translated outside research settings for on-demand health applications. By taking advantage of their ubiquity, smartphone-based systems could aid in the monitoring of breathing status of the general population, where this general practice remains unclear if we consider that these parameters are not always recorded on a daily basis even in clinical settings. The results obtained in this study point out the feasibility of developing a mobile system being able to provide information about instantaneous RR and tidal volume when calibrated on an individual basis. It is foreseen that when calibration is not possible to be performed, this smartphone approach could still be used as a qualitative indicator of changes in tidal volume due to the high correlation between the chest movement signal and tidal volume that reflects the major contribution of chest wall displacements to tidal volume. To this end, this paper reports our initial step towards the estimation of V_{T} from a surrogate signal obtained with a smartphone. We cannot make conclusions about the robustness in terms of measurement conditions such as gender, body mass index or lighting conditions given the small sample size and conditions tested. These will be explored in future studies.

Currently, we are running a study regarding an efficient, automated and easy-to-use calibration procedure that can be

performed with an incentive spirometer (IS). This is a low-cost off-the-shelf device which has the potential to be used in non-clinical settings. Briefly, by taking advantage of the high linear relationship between smartphone measurements and tidal volume, the calibration model is computed while breathing at only two reference volume points through the IS. Preliminary results have shown to be comparable to those presented in this paper which would allow a fast, automated and easy-to-perform calibration procedure with wireless remote controlling capabilities. In parallel, we are working on the implementation of the proposed signal processing techniques, currently developed for Android, on iOS to cover the two dominant smartphone operating systems. Nevertheless, the authors recognize that future work has to be done in order to make it feasible in practice; in particular, improvements should be done to replace the subject-by-subject calibration with a more generic one as well as to perform measurements under real-life conditions instead of restrictive settings. Future work of our research group includes study of body tracking and motion artifact algorithms to address some of the limitations mentioned earlier. Exploration of independent component analysis (ICA) and similar techniques intended to minimize motion artifacts are the topic of future work.

References

[1] F. Q. Al-Khalidi, R. Saatchi, D. Burke, H. Elphick, and S. Tan, "Respiration rate monitoring methods: A review," *Pediatr. Pulmonol.*, vol. 46, no. 6, pp. 523–529, Jun. 2011.

[2] M. A. Cretikos, R. Bellomo, K. Hillman, J. Chen, S. Finfer, and A. Flabouris, "Respiratory rate: The neglected vital sign," *Med. J. Aust.*, vol. 188, no. 11, p. 657, 2008.

[3] M. Folke, L. Cernerud, M. Ekström, and B. Hök, "Critical review of non-invasive respiratory monitoring in medical care," *Med. Biol. Eng. Comput.*, vol. 41, no. 4, pp. 377–383, Jul. 2003.

[4] B. M. Koeppen and B. A. Stanton, *Berne & Levy Physiology, Updated Edition*. New York, NY, USA: Elsevier Health Sciences, 2009.

[5] K. P. Cohen *et al.*, "Comparison of impedance and inductance ventilation sensors on adults during breathing, motion, and simulated airway obstruction," *IEEE Trans. Biomed. Eng.*, vol. 44, no. 7, pp. 555–566, Jul. 1997.

[6] G. B. Drummond, A. F. Nimmo, and R. A. Elton, "Thoracic impedance used for measuring chest wall movement in postoperative patients," *Br. J. Anaesth.*, vol. 77, no. 3, pp. 327–332, Sep. 1996.

[7] M. A. E. Ramsay, M. Usman, E. Lagow, M. Mendoza, E. Untalan, and E. De Vol, "The accuracy, precision and reliability of measuring ventilatory rate and detecting ventilatory pause by rainbow acoustic monitoring and capnometry," *Anesth. Analg.*, vol. 117, no. 1, pp. 69–75, Jul. 2013.

[8] J. J. Vargo, G. Zuccaro, Jr., J. A. Dumot, D. L. Conwell, J. B. Morrow, and S. S. Shay, "Automated graphic assessment of respiratory activity is superior to pulse oximetry and visual assessment for the detection of early respiratory depression during therapeutic upper endoscopy," *Gastrointest. Endosc.*, vol. 55, no. 7, pp. 826–831, Jun. 2002.

[9] K. Ashutosh, R. Gilbert, J. H. Auchincloss, J. Erlebacher, and D. Peppi, "Impedance pneumograph and magnetometer methods for monitoring tidal volume," *J. Appl. Physiol.*, vol. 37, no. 6, pp. 964–966, 1974.

[10] P. Grossman, M. Spoerle, and F. H. Wilhelm, "Reliability of respiratory tidal volume estimation by means of ambulatory inductive plethysmography," *Biomed. Sci. Instrum.*, vol. 42, pp. 193–198, 2006.

[11] A. Johansson and P. P. Å. Öberg, "Estimation of respiratory volumes from the photoplethysmographic signal. Part I: Experimental results," *Med. Biol. Eng. Comput.*, vol. 37, no. 1, pp. 42–47, Jan. 1999.

[12] Y. S. Lee, P. N. Pathirana, C. L. Steinfort, and T. Caelli, "Monitoring and analysis of respiratory patterns using microwave Doppler radar," *IEEE J. Transl. Eng. Health Med.*, vol. 2, pp. 1–12, Nov. 2014.

[13] G. Li *et al.*, "Quantitative prediction of respiratory tidal volume based on the external torso volume change: A potential volumetric surrogate," *Phys. Med. Biol.*, vol. 54, no. 7, pp. 1963–1978, Apr. 2009.

[14] M. R. Miller *et al.*, "Standardisation of spirometry," *Eur. Respir. J.*, vol. 26, no. 2, pp. 319–338, 2005.

[15] C.-L. Que, C. Kolmaga, L.-G. Durand, S. M. Kelly, and P. T. Macklem, "Phonospirometry for noninvasive measurement of ventilation: Methodology and preliminary results," *J. Appl. Physiol. Bethesda Md 1985*, vol. 93, no. 4, pp. 1515–1526, Oct. 2002.

[16] O. Sayadi, E. H. Weiss, F. M. Merchant, D. Puppala, and A. A. Armoundas, "An optimized method for estimating the tidal volume from electrocardiographic signals: Implications for estimating minute ventilation," *Amer. J. Physiol. Heart Circ. Physiol.*, vol. 307, pp. H426–H436, 2014.

[17] B. J. Semmes, M. J. Tobin, J. V. Snyder, and A. Grenvik, "Subjective and objective measurement of tidal volume in critically ill patients," *Chest*, vol. 87, no. 5, pp. 577–579, 1985.

[18] R. Gilbert, J. H. Auchincloss, J. Brodsky, and W. Boden, "Changes in tidal volume, frequency, and ventilation induced by their measurement," *J. Appl. Physiol.*, vol. 33, no. 2, pp. 252–254, Aug. 1972.

[19] B. A. Reyes, N. Reljin, and K. H. Chon, "Tracheal Sounds Acquisition Using Smartphones," *Sensors*, vol. 14, no. 8, pp. 13830–13850, Jul. 2014.

[20] F. Zhao, M. Li, Y. Qian, and J. Z. Tsien, "Remote measurements of heart and respiration rates for telemedicine," *PLoS One*, vol. 8, no. 10, p. e71384, Oct. 2013.

[21] L. Sherwood, *Fundamentals of Human Physiology*. 4th ed., Boston, MA, USA: Cengage Learning, 2011.

[22] M. Bartula, T. Tigges, and J. Muehlsteff, "Camera-based system for contactless monitoring of respiration," in *Proc. 2013 35th Annu. Int. Conf. IEEE Eng. Med. Biol. Soc.*, pp. 2672–2675.

[23] S. J. Cala *et al.*, "Chest wall and lung volume estimation by optical reflectance motion analysis," *J. Appl. Physiol.*, vol. 81, no. 6, pp. 2680–2689, Dec. 1996.

[24] M.-Z. Poh, D. J. McDuff, and R. W. Picard, "Advancements in noncontact, multiparameter physiological measurements using a webcam," *IEEE Trans. Biomed. Eng.*, vol. 58, no. 1, pp. 7–11, Jan. 2011.

[25] D. Shao, Y. Yang, C. Liu, F. Tsow, H. Yu, and N. Tao, "Noncontact monitoring breathing pattern, exhalation flow rate and pulse transit time," *IEEE Trans. Biomed. Eng.*, vol. 61, no. 11, pp. 2760–2767, Nov. 2014.

[26] L. Tarassenko, M. Villarroel, A. Guazzi, J. Jorge, D. A. Clifton, and C. Pugh, "Non-contact video-based vital sign monitoring using ambient light and auto-regressive models," *Physiol. Meas.*, vol. 35, no. 5, p. 807, 2014.

[27] H.-Y. Wu, M. Rubinstein, E. Shih, J. Guttag, F. Durand, and W. Freeman, "Eulerian video magnification for revealing subtle changes in the world," *ACM Trans Graph*, vol. 31, no. 4, pp. 65:1–65:8, Jul. 2012.

[28] K. Konno and J. Mead, "Measurement of the separate volume changes of rib cage and abdomen during breathing," *J. Appl. Physiol.*, vol. 22, no. 3, pp. 407–422, Mar. 1967.

[29] N. E. Huang *et al.*, "The empirical mode decomposition and the Hilbert spectrum for nonlinear and non-stationary time series analysis," *Proc. R. Soc. Lond. Ser. Math. Phys. Eng. Sci.*, vol. 454, no. 1971, pp. 903–995, 1998.

[30] P. Flandrin, P. Goncalves, and G. Rilling, "Detrending and denoising with empirical mode decomposition," in *Proc. Eur. Signal Process. Conf.*, 2004, vol. 2, pp. 1581–1584.

[31] L. Cohen, "Time-frequency distributions-a review," *Proc. IEEE*, vol. 77, no. 7, pp. 941–981, Jul. 1989.

[32] W. Martin and P. Flandrin, "Wigner–Ville spectral analysis of nonstationary processes," *IEEE Trans. Acoust. Speech Signal Process.*, vol. 33, no. 6, pp. 1461–1470, Dec. 1985.

[33] F. Hlawatsch, T. G. Manickam, R. L. Urbanke, and W. Jones, "Smoothed pseudo-Wigner distribution, Choi-Williams distribution, and cone-kernel representation: Ambiguity-domain analysis and experimental comparison," *Signal Process.*, vol. 43, no. 2, pp. 149–168, May 1995.

[34] Y. Sun, S. Hu, V. Azorin-Peris, S. Greenwald, J. Chambers, and Y. Zhu, "Motion-compensated noncontact imaging photoplethysmography to monitor cardiorespiratory status during exercise," *J. Biomed. Opt.*, vol. 16, no. 7, pp. 077010–077010, 2011.

[35] T. M. Baird and M. R. Neuman, "Effect of infant position on breath amplitude measured by transthoracic impedance and strain gauges," *Pediatr. Pulmonol.*, vol. 10, no. 1, pp. 52–56, 1991.

[36] M. J. Tobin, S. M. Guenther, W. Perez, and M. J. Mador, "Accuracy of the respiratory inductive plethysmograph during loaded breathing," *J. Appl. Physiol.*, vol. 62, no. 2, pp. 497–505, 1987.

[37] V. P. Vellody, M. Nassery, W. S. Druz, and J. T. Sharp, "Effects of body position change on thoracoabdominal motion," *J. Appl. Physiol.*, vol. 45, no. 4, pp. 581–589, Oct. 1978.

[38] W. S. Druz and J. T. Sharp, "Activity of respiratory muscles in upright and recumbent humans," *J. Appl. Physiol.*, vol. 51, no. 6, pp. 1552–1561, Dec. 1981.

Authors' photographs and biographies not available at the time of publication.